The use of direct boundary element method for gaining insight into complex seismic site response

Sonia Álvarez-Rubio [a,*], Juan José Benito [b], Francisco José Sánchez-Sesma [c], Enrique Alarcón [d]

[a] *Departamento de Matemática Aplicada, E.U.I.T. Industrial, Universidad Politécnica de Madrid, Ronda de Valencia, 3, 28012-Madrid, Spain*

[b] *Departamento de Ingeniería de Construcción y Fabricatión, E.T.S.I. Industriales, Universidad Nacional Distancia, Apdo. 60. 149, 28080-Madrid, Spain*

[c] *Instituto de Ingeniería, UNAM, Cd Universitaria, Apdo. 70-472, Coyoacán 04510, México D.F., México*

[d] *Departamento de Mecánica Estructural y Construcciones Industriales, E.T.S.I. Industriales, Universidad Politécnica de Madrid, José Gutiérrez Abascal, 2, 28006-Madrid, Spain*

Abstract

The boundary element method is specially well suited for the analysis of the seismic response of valleys of complicated topography and stratigraphy. In this paper the method's capabilities are illustrated using as an example an irregularity stratified (test site) sedimentary basin that has been modelled using 2D discretization and the Direct Boundary Element Method (DBEM).

Site models displaying different levels of complexity are used in practice. The multi-layered model's seismic response shows generally good agreement with observed data amplification levels, fundamental frequencies and the high spatial variability. Still important features such as the location of high frequencies peaks are missing. Even 2D simplified models reveal important characteristics of the wave field that 1D modelling does not show up.

Keywords: Site effects; Local conditions; Euroseistest; Numerical modelling; Boundary element method

1. Introduction

Local soil conditions play an important role on the modification of seismic ground motion. Therefore, their effects may become crucial in the selection or simulation of ground motion for use in structural seismic response analysis. The effects of surface geology can greatly enlarge the site response exerting an important influence on the distribution of damage observed during earthquakes. Refs. [1–7] are just examples of the vast bibliography devoted to the understanding of seismic site effects. Seismic codes are echoing the importance of site effects by approaching a more detailed quantification of soil effects [8]. Moreover, recent papers point out the need of incorporating or reviewing parameters related to the local topography to account for topographical effects in the seismic response [4–6].

In the last decades the evaluation of site effects was done via different approaches. The observations gathered after recent destructive earthquakes, as well as, the development of high quality dense networks, have made possible empirical site-response estimations which reveal remarkable effects of geological and topographical local conditions on the recorded ground motion. On the other hand, the ongoing progress in designing faster and more powerful computers have encouraged the adaptation of numerical techniques to local seismic response assessment.

Comparison between theoretical and empirical site-response estimations have lately been investigated throughout several works. There is some controversy on the discussion about agreement between results arisen from both approaches.

For instance, in [9] it is concluded that there is a good agreement between empirical data and theoretical results, concerning purely topographical induced amplifications on ridge tops. On the contrary, the authors of [10] pointed out a possibility of disagreement between, the HVSR empirical response (horizontal to vertical spectral ratio) and the theoretical transfer function, due to the fact that the 2D homogeneous model used in the work may be too simplified for the particular mountain investigated. This last discrepancy is discussed again in [11] in terms of the inadequacy of the 2D model used. In [12] a quantitative difference is also found between theoretical and observed amplifications at topographic features. That paper confirmed the conclusion noted by [13–16] which attributes the limitations of the theoretical simulations on complex sites, to the scarce information on underground irregular structure.

The authors in Ref. [17] have evaluated the use of the average 30-m shear-wave velocity and associated site classifications by comparing, two methods of estimating linear site amplification (the quarter-wavelength and the Haskell propagator matrix methods), to observed ground motion in sites in Los Angeles Region associated to mainshocks and aftershocks of the Northridge earthquake. Both methods predict the general trend of the observed site response, although there has been detected disparity between observed and theoretical amplification that could warrant caution when predicting site amplification. The authors discuss the large scattering of the correlation between results in terms of several factors such as the absence of information below 30 m, the propagation complexities contributing to the ground motions that are not accounted by the applied methods.

Therefore, according to the current situation, there are many factors that may probably contribute to this difference. A way of shedding light on the understanding of the site-response phenomena consists in developing high-performance numerical methods for simulations on complex sites. This issue is addressed, in this work, by the application of the Direct Boundary Element Method (DBEM) formulation, presented in [7,18], to a realistic site such as the Volvi Sedimentary Basin (Greece). It is a test-site where the geometry, dynamic properties and stratigraphy are well known. One of the main advantages of the DBEM is that it has been established to deal with 2D irregular sub and surficial topographies that shape complex laterally non-homogeneous media in presence of soft soils.

Theoretical approaches offer the possibility of handling the modelling of the site, so that different aspects of the phenomenon taking place can be investigated. In this respect, the simulations presented in this work, have been carried out on several models—with different level of detail—designed from the geological and topographical information published [19–21]. The complex ones exhibit an irregular multi-layered media. But, since one of the main problems on site-effect studies is that, detailed underground geological and topographical structure is rarely known, simplified approaches should remain to be useful tools for site-response estimation. Therefore, one-layered models of the Volvi basin have been investigated in order to evaluate the trade-off between, complexity and computing-time-consumptions of the numerical model, and the reliability of the simulation. In all cases the site-response estimated corresponds to the vertical incidence of a unit amplitude SV wave, ranging up to 5 Hz.

The work has been focused to investigate some of the aspects that characterize site effects: topographic and soil amplification, spectral content, ground motion variability, etc... Some correlation have been found between those aspects and relevant features of the models which confirm conclusions of other researchers. It also can be concluded that the DBEM is a suitable technique for parametric studies in order to investigate the main features of local conditions that should be taken into account to improve modem seismic code provisions.

2. Methodology: 2D site effects computation using DBEM

2.1. *DBEM time-harmonic formulation*

As it is well known there are many engineering topics where boundary element methods (BEM) have been applied, for instance some recent works can be seen in [22–24]. Issues such as the reduction of dimensionality, the fulfillment of radiation conditions at infinity, and the high accuracy of results, make this technique attractive in engineering seismology and especially in site effects assessment. Detailed study of the technique's formulation has been extensively addressed in the literature (e.g. [25–32]). The main goal of this paragraph is to give an overview of the adaptation of the DBEM to the computation of the local site response in laterally varying stratified media, presented in [7,18].

The basic boundary element integral equation for the frequency domain study of a viscoelastic region D (with ∂D as its boundary), is the following displacement representation for a point i on ∂D:

$$\mathbf{c}^i\mathbf{u}^i + \int_{\partial D} \mathbf{t}^*\mathbf{u}\,\mathrm{d}S = \int_{\partial D} \mathbf{u}^*\mathbf{t}\,\mathrm{d}S, \tag{1}$$

where $\mathbf{u}$ and $\mathbf{t}$ = displacement and traction vectors, respectively, whereas $\mathbf{u}^*$ and $\mathbf{t}^*$ = fundamental solution tensors corresponding to a point load in the infinite domain. The coefficient $\mathbf{c}^i$ depends only on the boundary geometry at point "i".

Once the boundary ∂D is discretized into N constant elements—in [7,18] this approach has been validated for site effects assessment, expression (1) yields the following system of equations:

$$\mathbf{Hu} = \mathbf{Gt}, \tag{2}$$

where $\mathbf{H}$ and $\mathbf{G}$ are the coefficient matrices obtained by integration over the elements, and $\mathbf{u}$ and $\mathbf{t}$ are the vectors containing the nodal displacement and traction values, respectively.

2.2. DBEM site effects estimation

The DBEM has been applied and validated for the computation of seismic response at 2D site models [7,18], which represent irregular stratified media. The established problem is as follows: given a model of the site, see Fig. 1, which is subjected to seismic motion, the total wave field is written in terms of the total displacement ($\mathbf{u}^t$) and total tractions ($\mathbf{t}^t$) as

$$\begin{aligned} \mathbf{u}^t &= \mathbf{u}^0 + \mathbf{u}^d, \\ \mathbf{t}^t &= \mathbf{t}^0 + \mathbf{t}^d. \end{aligned} \tag{3}$$

$(\mathbf{u}^0, \mathbf{t}^0)$ is the *free-field* that is, the primary waves in the absence of irregularities. It is analytically known and, in this work it is taken as the solution of the transmission and reflection of the in-plane problem (P–SV waves) at the free surface and boundaries of the homogeneous half-space ($z \leqslant 0$). The *diffracted field* is denoted by $(\mathbf{u}^d, \mathbf{t}^d)$, and it is generated by the interference between the primary waves and the irregularities of the soil. The fulfillment of the compatibility and equilibrium conditions turns the problem to a Neumann one (displacements are the unknowns). To solve the problem two situations have to be considered depending on the local conditions: the *internal and the external problem* [28]. When the internal problem is being solved—for instance in layers II and III of Fig. 1—the radiation condition of the actual problem is satisfied and, according to expression (2) the DBEM's formulation is established as

$$H\mathbf{u}^t = G\mathbf{t}^t. \tag{4}$$

Whereas, when the external problem is under study, e.g. the rock basement (layer I) in Fig. 1, DBEM's implementation is done in terms of the diffracted field, that is

$$\begin{aligned} H\mathbf{u}^d &= G\mathbf{t}^d, \\ H(\mathbf{u}^t - \mathbf{u}^0) &= G(\mathbf{t}^t - \mathbf{t}^0). \end{aligned} \tag{5}$$

An expanded matrix formulation and a more detailed explanation of the application of expressions 4 and 5 can be seen in [7,18]. In the next sections the results of the computation of the seismic response at an alluvial basin, are analyzed.

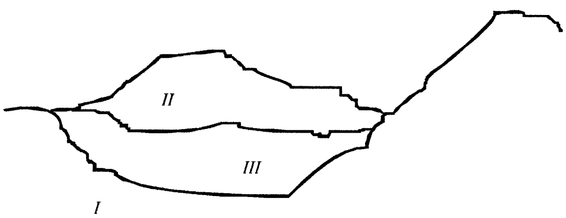

Fig. 1. An example of a site model representing a multi-layered region defined by irregular sub and surficial boundaries.

3. Modelling of the Volvi sedimentary basin

3.1. Local conditions at the basin

The Volvi sedimentary basin, known in site effects studies as the European test-site EUROSEISTEST, is located between the Lagada and Volvi lakes in the Mygdonian graben some 30 km to the East of Thessaloniki in Northern Greece. It is a seismically and tectonically active region [33]; the epicenters of the destructive Thessaloniki earthquake sequence in 1978 are situated near the city of Profitis, see Fig. 2. It is a 6 km wide and 200 m deep basin with a very well determined subsoil structure, due to the numerous geophysical and geotechnical investigations that have taken place in the valley [19,21,34]. A detailed cross-section of the site is shown in Fig. 3. The site is irregularly stratified and sharply limited by four major faults (I–IV) which, as it will be discussed later, play an important role in the seismic response of the basin. The properties of the materials composing the structure are shown in Table 1 (ρ: density, β: S-wave velocity, ν: Poisson's ratio, α: P-wave velocity, Q_S: S-quality factor). The results evaluated further on, are checked against others arisen from empirical techniques applied to data recorded at networks deployed during different periods of time.

3.2. Basin modelling

People involved in hazard and seismic risk analysis are aware of the importance of including site effects in their analysis. From a practical point of view, investigations

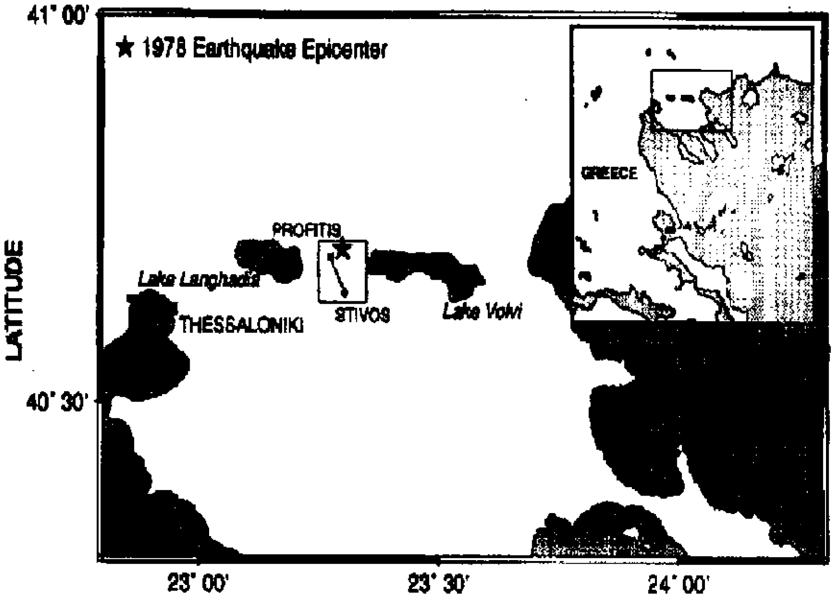

Fig. 2. Map of the location of the EUROSEISTEST. The NNW-SSE 2D soil structure of the basin depicted in Fig. 3, is represented, in this figure, by the line that joins Profitis (PRO) site to Stivos (STE) site.

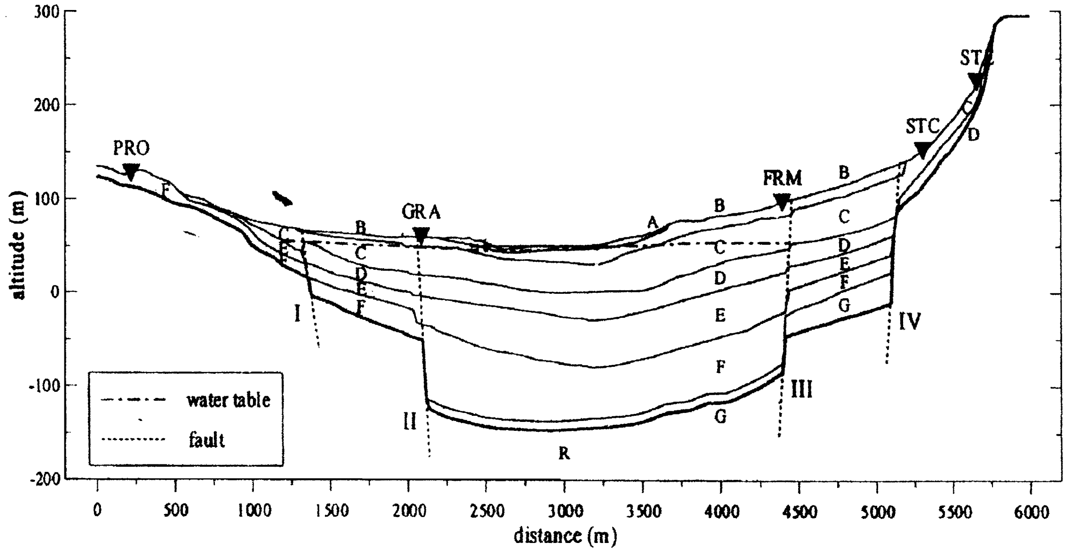

Fig. 3. The structure corresponds to a cross-section of the Volvi sedimentary basin close to the city of Thessaloniki in Greece [20]. This basin's structure is denoted in this work as *model I*. It can be seen some of the stations deployed for wave field observation [34,35].

should be focused as to provide a deeper insight of the complex phenomena relying on few parameters that could characterize realistically the seismic response of the site. Numerical techniques can play an important role through the modelling process: site subsoil structure models of different degree of detail, based on the available information, can reveal relevant parameters for site response quantification.

For that purpose in this work we present the seismic response computed along the surface of different basin models. The different meshes have been designed with the intention of investigating the effects of the main features describing the laterally irregular soil layers within the basin: basin geometry, material properties, and sharply laterally irregular discontinuities between layers.

Table 1
Material's properties in the model of Fig. 3

Layer	ρ (kg/m^3)	β (m/s)	Poisson's ratio	α (m/s)	Q_s[a]
A	1700	130	0.408	330	40
B	1800	200	0.375	450	20
C	1800	300	0.290	550	30
D	2100	450	0.285	820	25
E	2150	650	0.285	1185	50
F	2200	900	0.285	1640	60
G	2500	1250	0.280	2260	100
R	2600	2500	0.277	4500	200

[a] Q_s value at the reference frequency of 1 Hz.

Table 2
Properties of the materials that compose the six layers of the model shown in Fig. 4

Layer	ρ (kg/m^3)	β (m/s)	v	α (m/s)	Q_s[a]
1	2600	2500	0.277	2260	200
2	1800	250	0.332	498	25
3	2100	450	0.285	820	25
4	2150	650	0.285	1185	50
5	2200	900	0.285	1640	60
6	2500	1250	0.280	4500	100

[a] Q_s value at the reference frequency 1 Hz.

The models have been based on digitized 2D valley's structure in Fig. 3, *model I*, and soil properties of Table 1. The first model, *model II*, is shown in Fig. 4a. The difference between the structures in Figs. 3 and 4a is that layers A, B and C (model 1) are merged into layer 2 (model II). Table 2 shows the soil properties of the latter. The material properties assigned to layer 2 (model II) correspond to the mean values of layers A, B and C (model I).

One of the pitfalls of site effect assessment is the lack of information about local conditions at a site. Therefore, *models III* and *IV* (Fig. 5) have been used to evaluate the level of representativeness of the seismic response computed when only simplified models are available. Both are one-layer structures (layer 2), whose dynamic properties are shown in Table 3 and they are the mean value of the properties of layers 2–6 in model II. There are differences between them; the irregularities at the surface and at the interface between rock basement (layer 1) and layer 2 has been kept on model III. Whereas on model IV these irregularities have been smoothed.

3.3. Mesh generation

The generation of the mesh for all models is based on the constant elements boundary discretization, that has been previously validated for site effects assessment [7,18]. Hereinafter the simulations carried out are related to the vertical incidence of a SV-wave (amplitude unit) on the rock basement (layer 1), over a spectral band up to 5 Hz. The lengths of the elements (L_{el}) where obtained taking into account the relation between the

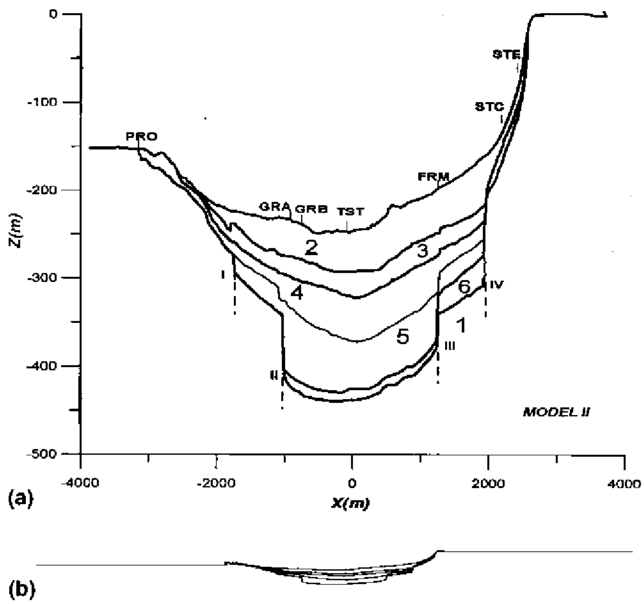

Fig. 4. (a) Multi-layered structure of the Volvi sedimentary basin analysed in this work and denoted by *model II*. It has been obtained by the digitation of model I in Fig. 3. (b) In the figure it can be seen the dimension of the free surface extended on both sides of the valley (2:1 x:y-scale).

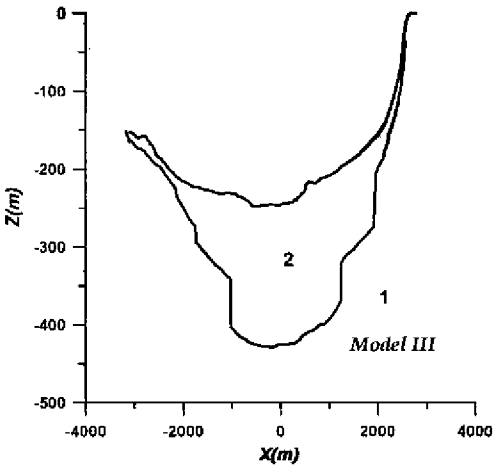

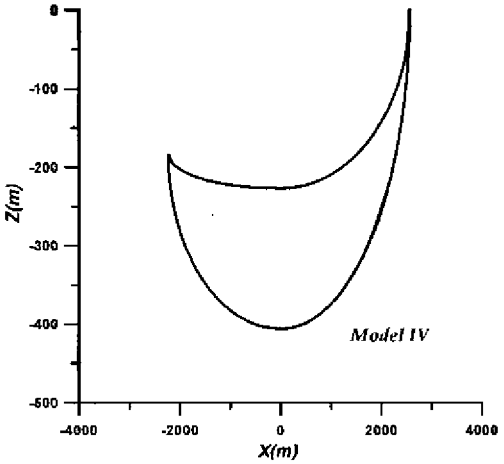

Fig. 5. Homogeneous models of the Volvi sedimentary basin analyzed. The boundaries in *model III* have been kept irregular; while in *model IV* have been smoothed.

Table 3
Properties of the materials in models III and IV

Layer	ρ (kg/m^3)	β (m/s)	ν	α (m/s)	Q_s^*
1	2600	2500	0.277	4500	200
2	2143	692	0.299	1718	53

minimum wavelength, $\lambda_{\min}$, the minimum S-wave velocity of the site, $\beta_{\min}$, and the maximum computation frequency, $f_{\max}$:

$$\lambda_{\min} = \beta_{\min}/f_{\max}. \tag{6}$$

It has been observed that the method is a stable, robust and free of edge effects technique, see [7,18], when the lengths of the elements are optimized to the value:

$$L_{\mathrm{el}} = \lambda_{\min}/5. \tag{7}$$

For model II and in the band up to 2.5 Hz the length is L_{el} = 20 m, whereas for (2.5, 5) Hz L_{el} = 10 m. In simulations carried over models III and IV the length is L_{el} = 20 m. In both borders of the valley, the free surface is extended to the total length of the interface between the rock basement (layer 1) and layer 6, see Fig. 4b. The heaviest computation is performed over a discretized mesh composed of 5996 nodes.

The results achieved are depicted in terms of the horizontal displacement transfer functions $|Ux|$. These amplitudes represent the amplification factor *soil/unit incident amplitude*. In the comparison with other published results, it has to be taking into account that, amplification can be referred as *soil/reference station PRO*.

4. Computation of the basin site response

Transfer functions computed along the surface of the Graben's models have been analyzed within the framework of other results coming from data recorded at the site and other numerical investigations [1,34,35].

4.1. Multi-layered structure (model II)

In Fig. 6 some of the results of simulations carried out in model II are shown. It is interesting to see that the significant amplification occurring at the centre of the valley fits well with the observations. Horizontal amplification factors around 20, are found at about 0.8–1 Hz, that corroborates conclusions reported from data [34]. In Fig. 7a it can be seen this high amplification quantified in [35] by empirical techniques (standard spectral ratio relative to reference station PRO) at stations GRA, GRB, TST, FRM on the centre of the valley. These large peaks are in the range of the fundamental frequency of a layer of the same depth as the valley and properties of layer 2 in models III and IV. But their discontinuous distribution (see Fig. 7b) where the distortion of the 1D natural frequency is shown, reveal the 2D nature of the problem. This variability on the spatial amplification distribution tends to increase with frequency.

Spectra amplitudes in Fig. 8 corroborate qualitatively empirical results concerning this complex pattern amplification. The significant effects provoked by the sharp limits of the basin bordered by faults I–IV are clearly seen. It has been reported [34] that the inhomogeneous fault zone could be the source of focusing and special diffraction effects, that can be revealed as high amplitudes at sites located close to the faults, amplification occurring at high frequencies affecting the center of the basin,... The present numerical results reveal some of those features, e.g., in Fig. 6 and more clearly in Fig. 8, it is seen that, as it is concluded in [35] and shown

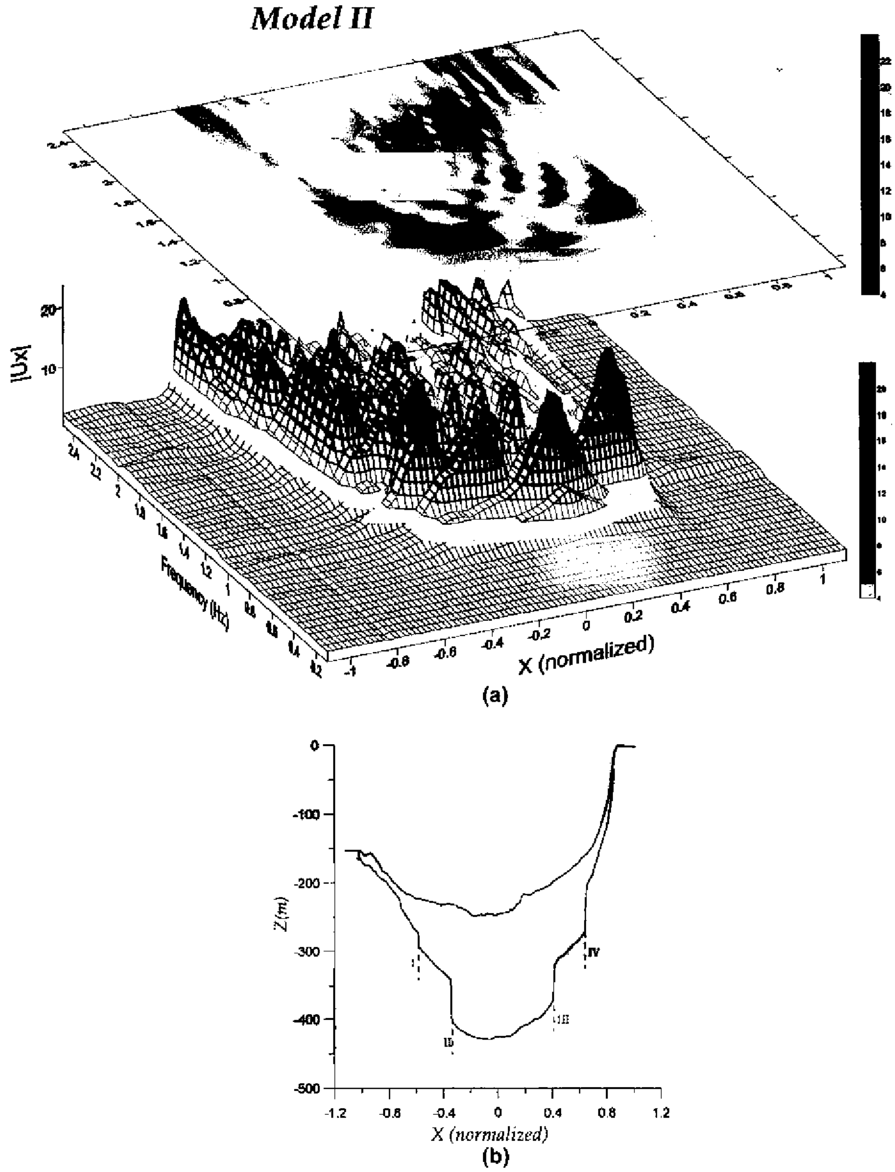

Fig. 6. Numerical seismic response computed on model II for vertical incidence of SV (amplitude unit) on the rock basement. (a) In OZ axis it is represented the amplitudes of the horizontal spectral displacements assessed for the free surface. (b) The x normalized coordinate is depicted.

in Fig. 7a, high resonant frequencies of the wave-field response are shifted toward the edges of the valley. Notice the amplification at the edges of the basin (STC, STE) for frequencies higher than 1.5 Hz.

This last specific characteristic of the seismic response has been underestimated in other numerical studies using a standard finite-difference method [1], where the authors pointed out that it could be due to several reasons concerning the simplification of models: the non-existing surface weathered layer in their model, some neglected thin layers, the smoothing of the inhomogeneous fault zone, more complex 3D effects,... In the same work the authors performed a more complex computation of the response of the basin applying a hybrid method to account for a more realistic incident wave field. In it they found that the amplification levels for frequencies higher than 1 Hz is better modeled. Following the conclusions in [1] and this study, it could be inferred that these high amplifications at the edges can be assessed more reliably by a combination of a more

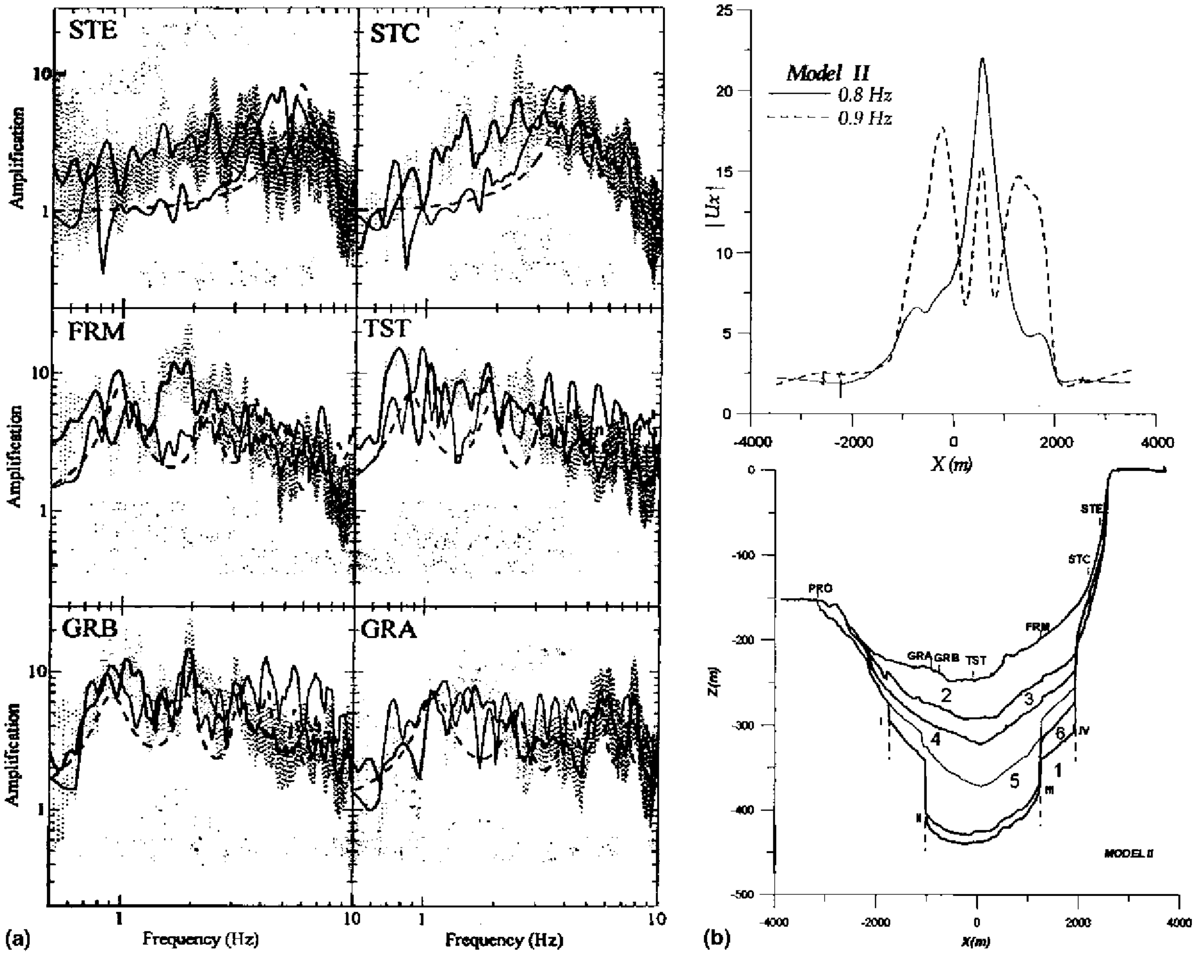

Fig. 7. (a) Comparison of observed and computed transfer functions obtained in [35]. Thick solid lines: average ratios of the transversal component of motion, relative to the corresponding component recorded at PRO. The shaded area shows the average plus or minus one standard deviation. Thin solid line: numerical transfer function, relative to the receiver at the location of PRO, obtained from the 2D finite-difference computations. Dotted line: numerical transfer function, relative to the receiver at the location of PRO, obtained from the 1D vertical profile at the location. (b) Horizontal transfer functions obtained on the free surface of model II for low frequencies (same radiation conditions as in Fig. 6).

realistic: geometry of the near-surface soil—as the one shown in model II, and of the incident radiation on the rock basement (to be performed in future works).

It is noticeable that amplitudes of the computed transfer functions in the higher frequency range, are larger than those of the observations. This issue is also shown in [35] where it is suggested that it could be due to a misfit of the Q values of the model, more than to a numerical instability of the technique used.

On the other hand, the computed transfer functions underestimate the amplification level observed at the centre of the valley for frequencies higher than 1.5 Hz. Taking into consideration the above remarks of the survey carried out in [1] this misfit could be explained in terms of the above mentioned neglected surface layers (soft and weathered layers). This issue is to be investigated in forthcoming works.

Regarding other characteristics of the seismic response computed, Fig. 9 displays the horizontal transfer functions across the basin versus the vertical component. It has been observed that as the frequency increases the vertical component of the motion undergoes significant amplification in comparison to the horizontal component. This issue once more attracts attention on the empirical technique of H/V (horizontal to vertical) ratio for site effects assessment. The reliability of this technique has being long discussed due to the underlined hypothesis of non-site effects on the vertical component. In Fig. 9 it is shown that in complex sites this assumption should be regarded with caution.

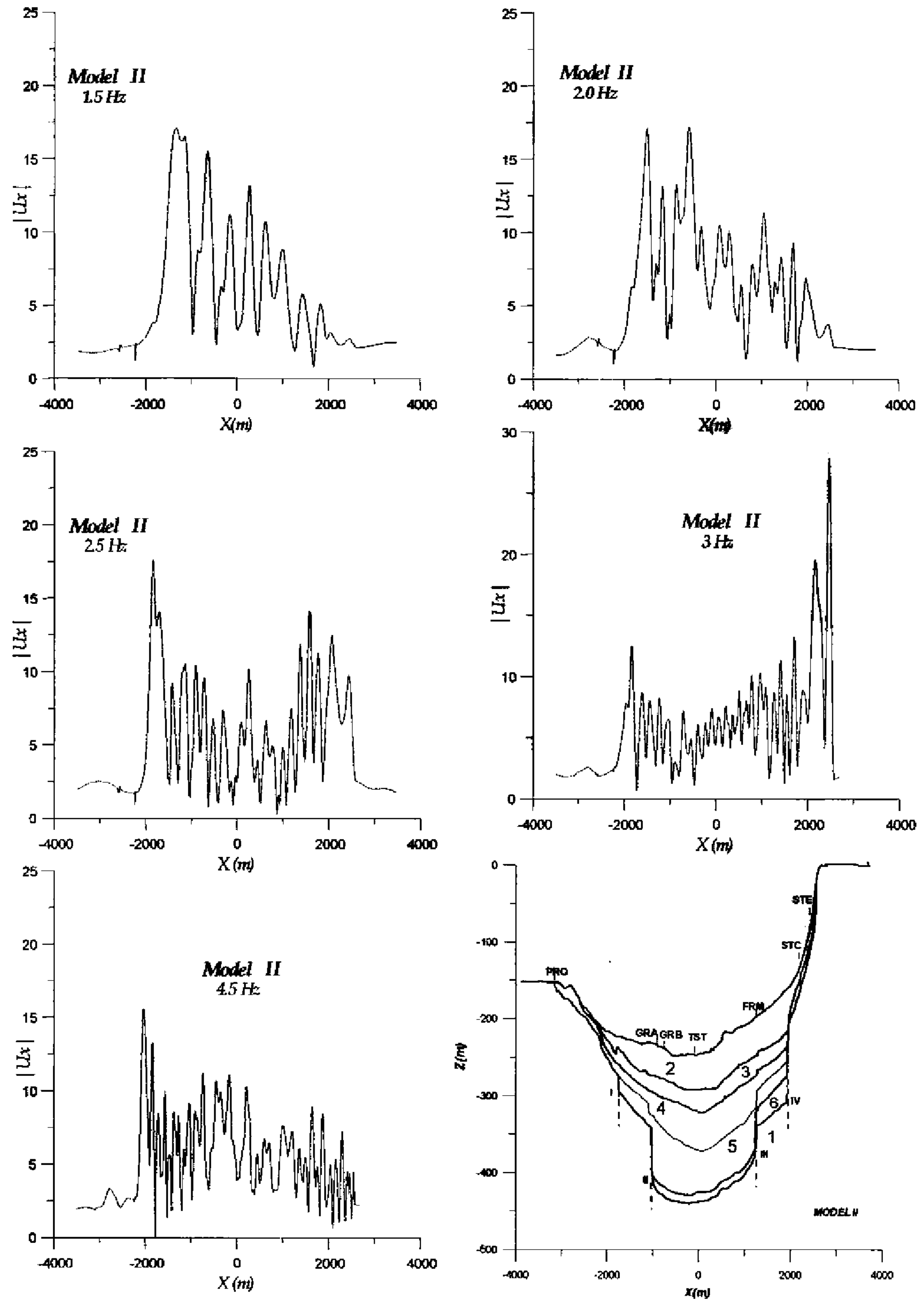

Fig. 8. Horizontal transfer functions obtained on the free surface of model II (same radiation conditions as in Fig. 6).

4.2. Homogeneous structure (models III and IV)

Fig. 10 displays the comparison between the transfer functions computed at low frequencies in models II–IV. It is shown that the center of the valley remains subjected to a low fundamental frequency in the range of 0.8–1 Hz in all models. It is relevant to see in Fig. 10 that there is a difference between results in the complex

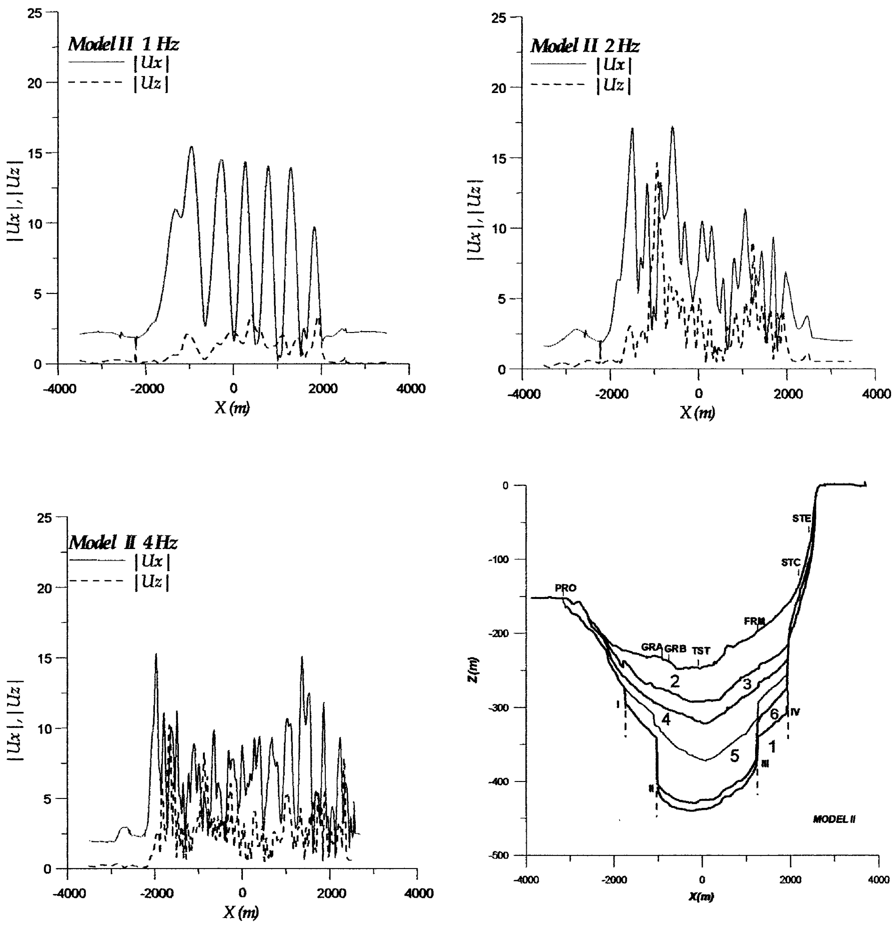

Fig. 9. Comparison of horizontal and vertical transfer functions obtained on the free surface of model II (same radiation conditions as in Fig. 6).

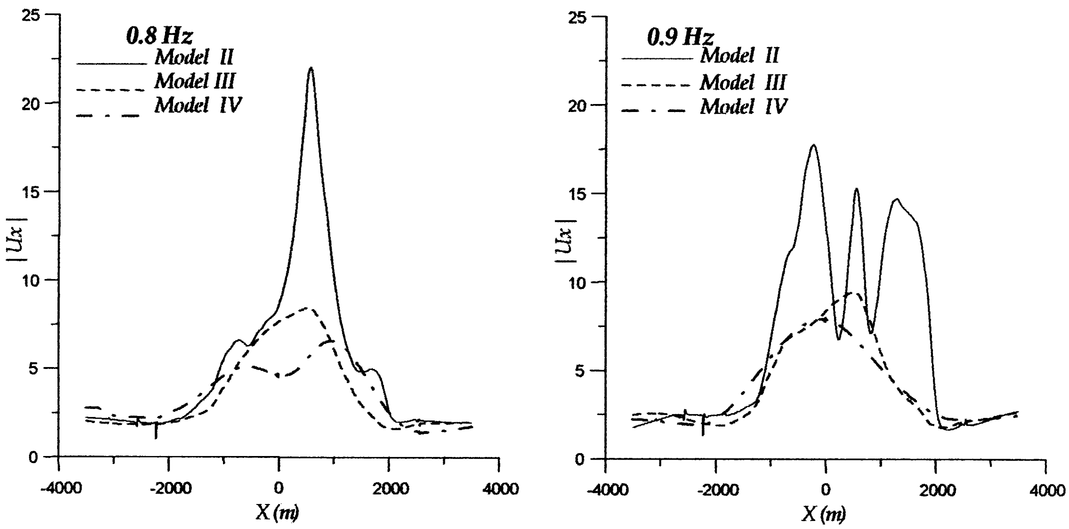

Fig. 10. Comparison between the horizontal transfer functions computed at low frequencies in models II–IV (same radiation conditions as in Fig. 6).

model, where the 2D effects slightly appear at 0.9 Hz and, homogeneous models where 1D effects remain predominant. It could be concluded that, apart from the expected lower fundamental amplification level at models III and IV—amplification around 10—in contrast to above mentioned level in model II—amplification around 20, the discontinuous distribution of the wave motion is influenced by the existence of stratified media.

An example of the seismic response is shown in Fig. 11 where it can be observed that, the spatial asymmetry pointed out in the preceding paragraph for model II, still remains in model III, but it disappears in model IV: the edges of the basin in model II produce asymmetric amplification which is maintained in model III and vanishes in model IV. Taking into account that the differences between the homogeneous models lies in the irregularities of the interface between layers 1 and 2 in model III, as opposite to the smoothness in model IV, the important role of the sub–surficial topography in the spatial distribution of the seismic response is clearly seen.

Coming back to one of the main aims of this analysis—i.e., the reliability of simple models if geometrical and dynamical information at the site is lacking—Figs. 12 and 13 show the computations in the homogeneous models as it was done in Fig. 6 for model II. It can be concluded that even with simple models as model IV, 2D modelling reveal the main characteristics observed in data, such as the amplification at the edge of the basin, which does not appear in 1D modelling. Also

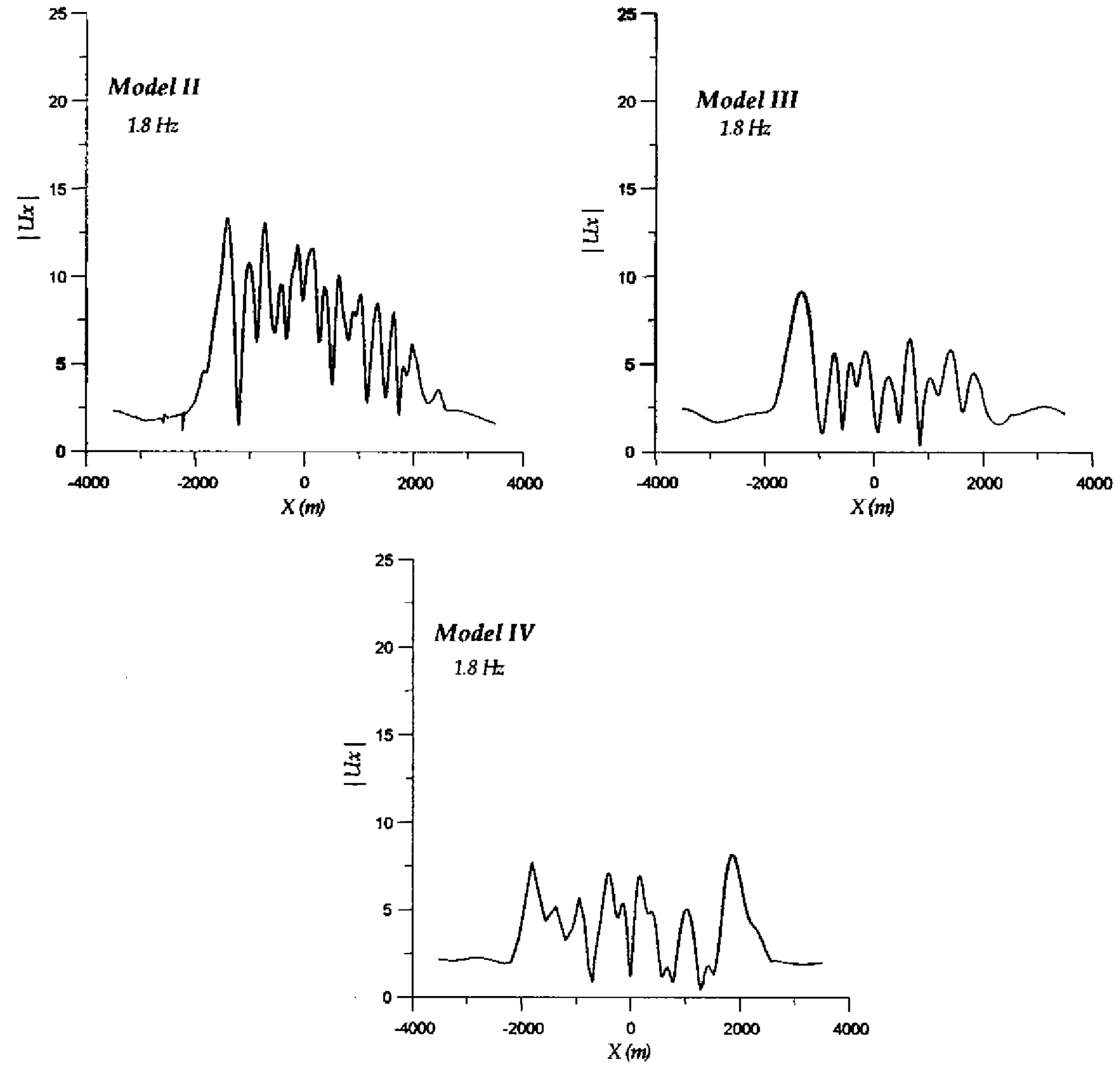

Fig. 11. Comparison between the horizontal transfer functions computed at 1.8 Hz in models II–IV (same radiation conditions as in Fig. 6).

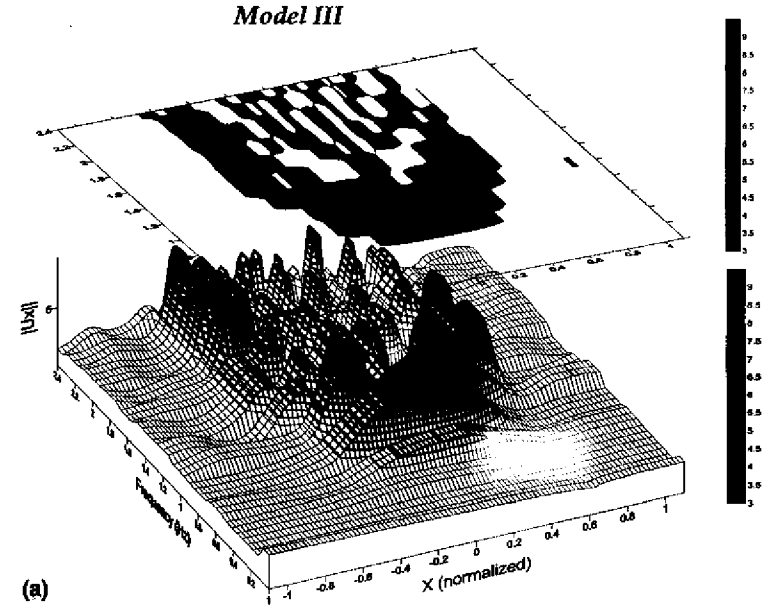

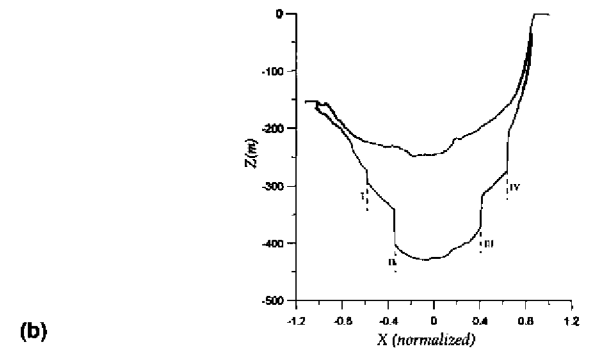

Fig. 12. Numerical seismic response computed on model III (same radiation conditions as in Fig. 6). (a) In OZ axis it is represented the amplitudes of the horizontal spectral displacements assessed for the free surface of model III. (b) The x normalized coordinate is depicted.

interesting is the influence of sharp irregularities such as the faults I–IV that affect the spatial distribution of the higher peaks. Therefore, simple 2D site effects assessment is a step forward to improve 1D modelling results for seismic design purposes.

5. General discussion and conclusions

Building codes are lately being revised as to include a finer and more realistic quantification of site effects. Modifications for design purpose should be included in terms of few parameters that can characterize reliably the ground motion at the site. Intending to approach this goal, in this work the Direct Boundary Element Method (DBEM) has been applied to the computation of seismic response at a complex sedimentary basin: the European test-site EUROSEISTEST. This technique is very attractive for site effects assessment due to its well known characteristics: the highly accurate solutions in the boundary and domain in spite of only establishing the equations and unknowns at the boundaries, and the suitable treatment of infinite, semi-infinite or very large regions, based on the fulfillment of the radiation conditions. Taking advantage of the technique's capacity to deal with realistic irregular sub and surficial topography, in combination of the detailed knowledge of the basin's geometrical and dynamical properties, the seismic response has been computed in models that display different levels of complexity: multi-layered and homogeneous models. The analysis of the results have made feasible to have a deeper insight into the nature of site effects.

As to the wave field computed in the multi-layered model is considered, results show good agreement on

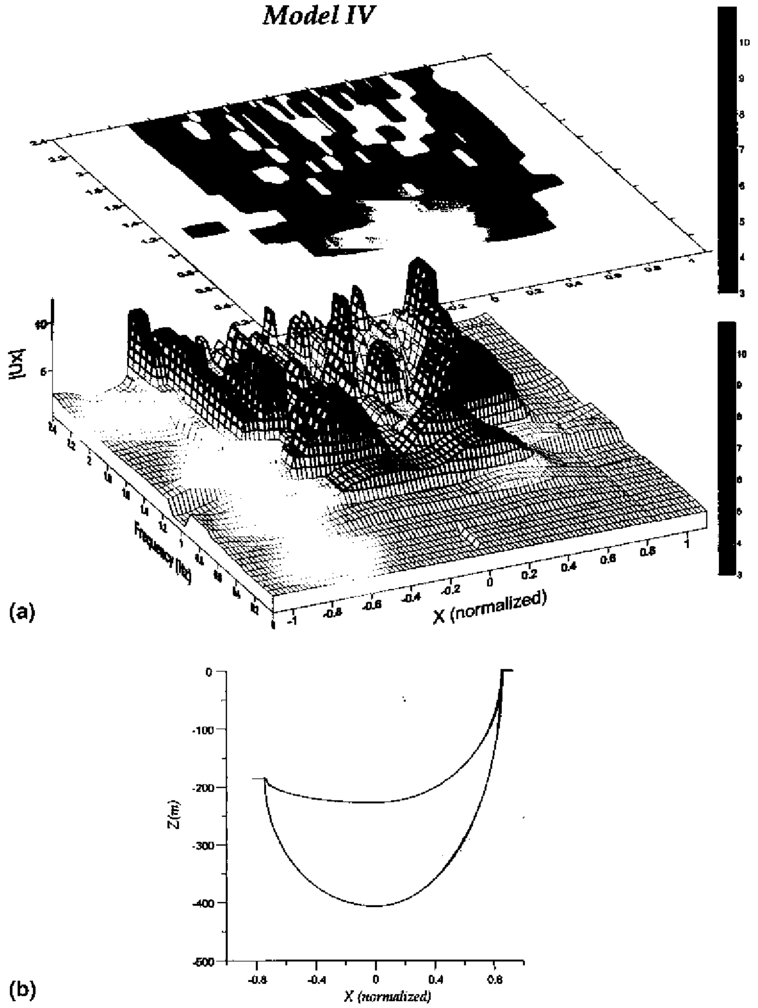

Fig. 13. Numerical seismic response computed on model IV (same radiation conditions as in Fig. 6). (a) In OZ axis it is represented the amplitudes of the horizontal spectral displacements assessed for the free surface of model IV. (b) The x normalized coordinate is depicted.

the amplification level regarding the fundamental frequency that affects the central part of the basin, as well as, other local peaks of amplification at higher frequencies at the edges of the basin. The complexity on the spatial variability of the wave field observed in the data recorded at the site is well revealed, but the particular location of the peaks, especially at high frequencies, is missing. This last issue should have to be improved because it can be of a great importance, especially in microzonation studies.

The investigation on the homogeneous models reveals the obvious underestimation of the soil amplification due to the simplified dynamic properties of the models, but still and from a conservative point of view, in the usual situations where the information of the site is scarce, these approaches are useful to determine the mean level of amplification as well as the fundamental frequency at low frequencies for seismic design purposes. It can be also inferred that some of the main features of the spatial variability, that strongly depend on the geometrical features of the rock basement topography, can be revealed. Therefore, 2D simple models (which are affordable from an economical point of view), contribute to improve the 1D modelling, by incorporating new aspects that will have effects on the assessment of ground motion characteristic parameters, e.g., the duration of the signal which is at present one of the targets under survey for different topographical irregularities.

Apart from the results about the quantification of site effects derived from this work, other interesting conclusions in relation to the nature of the different aspects of site effects—methodology and its future development—have been derived. It is seen that seismic site effects denote different physical phenomena due to the wave propagation of seismic waves through near-surface geological layers or/and geometrically irregular structures. An effect of these irregularities is *soil amplification* due to the impedance contrast between layers that affect a broad area of the site at low frequencies, and is locally distributed for higher frequencies. On the other hand the wave field at marked 2D geometries shows a strong *spatial variability* due to the main geometrical irregularities.

From a methodological point of view, other investigations have to be accomplished. The results here presented correspond to the propagation of a vertical SV wave. Further work is still needed to assess the influence of wave types and their incidence directions. The out-of-plane excitation, the heterogeneity and non linear issues have to be regarded as well. The work presented should be extended and parametric surveys on other relevant sites have to be performed. Special cases need to be covered in order to gain more information for code provisions purposes. Certainly, a significant need to be fulfilled is to accomplish the 3D modelling for complex sites. In any event, all these tasks may enhance our insight on local site response but the very random nature of the problem has to be regarded as well.

References

[1] Riepl J, Zahradnik J, Plicka V, Bard P-Y. About the efficiency of numerical 1-D and 2-D modelling of site effects in basin structures. Pure Appl Geophys 2000;157: 319–42.

[2] Álvarez-Rubio S. The local effect on the seismic soil displacement phenomemology and recent results [in Spanish]. In: Universidad Complutense de Madrid, editors. Física de la tierra, vol. 11. Madrid; 1999. p. 141–73.

[3] Sánchez-Sesma FJ, Madariaga R, Irikura K. An approximate elastic two-dimensional Green's function for a constant-gradient medium. Geophys J Int 2001;146: 237–48.

[4] Makra K, Raptakis D, Chávez-García FJ, Pitilakis K. How important is the detailed knowledge of a 2D soil structure for site response evaluation? In: Proceedings of the 12th European conference on earthquake engineering. London; 9–13 September 2002.

[5] Faccioli E, Vanini M, Frassine L. "Complex" site effects in earthquake ground motion, including topography. In: Proceedings of the 12th European conference on earthquake engineering. London; 9–13 September 2002.

[6] Paolucci R. Amplification of earthquake ground motion by steep topographic irregularities. Earthquake Eng Struct Dyn 2002;31:1831–53.

[7] Álvarez-Rubio S, Benito JJ, Sánchez-Sesma FJ, Alarcón E. The direct boundary element method: 2D site effects assessment on laterally varying layered media (methodology). Soil Dyn Earthq Eng 2004;24:167–80.

[8] Sabetta F, Bommer J. Modification of the spectral shapes and subsoil conditions in EUROCODE 8. In: Proceedings of the 12th European conference on earthquake engineering. London; 9–13 September 2002.

[9] Pederesen H, Le Brun B, Hatzfeld D, Campillo M, Bard P-Y. Ground-motion amplitude across ridges. Bull Seism Soc Am 1994;84:1786–800.

[10] Chávez-García FJ, Sánchez LR, Hatzfeld D. Topographic site effects and HVSR. A comparison between observations and theory. Bull Seism Soc Am 1996;86:1559–73.

[11] Chávez-García FJ, Rodríguez M, Field EH, Hatzfeld D. Topographic site effects. A comparison of the two nonreference methods. Bull Seism Soc Am 1997;87:1667–73.

[12] Paolucci R, Faccoli E, Maggio F. 3D response analysis of an instrumented hill at Matsuzaki, Japan, by a spectral method. J Seismol 1999;3:191–209.

[13] Geli L, Bard P-Y, Jullien B. The effect of topography on earthquake ground motion: a review and new results. Bull Seism Soc Am 1988;78:42–63.

[14] Spudich P, Hellweg M, Lee WHK. Directional topographic site response at Tarzana observed in afterShocks of the 1994 Northridge, California, Earthquake: implications for main shock. Bull Seism Soc Am 1996;86:S193–208.

[15] Bouchon M, Barker JS. Seismic response of a hill, the example of Tarzana, California. Bull Seism Soc Am 1996;86:66–72.

[16] Le Brun B, Hatzfeld D, Bard P-Y, Bouchon M. Experimental study of the ground motion on a large scale topographic hill at Kitherion (Greece). J Seismol 1999; 3(1):1–15.

[17] Wald LA, Mori J. Evaluation of methods for estimating linear site-response amplifications in the Los Angeles region. Bull Seism Soc Am 2000;90(6B):S32–42.

[18] Álvarez-Rubio S. Application of boundary element method to the seismic local effect quantification [in Spanish]. PhD Thesis, Escuela Técnica Superios de Ingenieros Industrials, Universidad Politécnica de Madrid, Spain; 2001.

[19] Jongmans D, Pitilakis K, Demanet D, Raptakis D, Riepl J, Horrent C, et al. EURO-SEISTEST: determination of the geological structure of the volvi basin and validation of the basin response. Bull Seism Soc Am 1998;88:473–87.

[20] Faccioli E, Paolucci R, Vanini M. TRISEE 3D site effects and soil-foundation interaction in earthquake and vibration risk evaluation. In: European Commission, Directorate General XII for Science, Research and Development 1994–1998 Environments and Climate Programme-Climate and Natural Hazards Unit.

[21] Raptakis D, Chávez-García FJ, Makra K, Pitilakis K. Site effects at Euroseistest—I. Determination of the valley structure and confrontation of observations with 1D analysis. Soil Dyn Earthq Eng 2000;19(1):1–22.

[22] Domínguez J. Boundary element method for simulation of wave propagation. In: Chouw N, Schmid G, editors. Wave propagation moving load, vibration reduction Wave 2000. Roterdam: Balkema; 2000. p. 337–55.

[23] Sáez A, Domínguez J. BEM analysis of wave scattering in transversely isotropic solids. Int J Num Meth Eng 1999;44: 1283–300.

[24] Alarcón E, Domínguez J, Fraile A. The boundary element method in soil mechanics [in Spanish]. In: Ministerio de Fomento, CEDEX, SEMSIG, editors. Homenaje a J.A. Jimenez Salas. Geotecnia en el año 2000. Madrid; 2000.

[25] Domínguez J, Alarcón E. Elastodynamics. In: Brebbia CA, editor. Progress in boundary element methods. London, Plymouth: Pentech Press; 1981.

[26] Domínguez J, Abascal R. Seismic response of strip footings on zoned viscoelastic soils. J Eng Mech 1989;115(5): 913–34.

[27] Maeso O, Aznárez JJ, Domínguez J. Effects of space distribution of excitation on seismic response of arch dams. J Eng Mech 2002;128(7):759–68.

[28] Domínguez J. Boundary elements in dynamics. Computational Mechanics Publications/Elsevier Applied Science; 1993.

[29] Gaul L, Kögl M, Wagner M. Boundary element methods for engineers and scientists. An introductory course with advanced topics. Berlin: Springer-Verlag; 2003.

[30] Wolf JP. The scaled boundary finite element method. New York: John Wiley; 2003.

[31] Boundary element XXV. Brebbia CA, Poljak D, Roje V, editors. Advances in boundary elements, vol. 18. WIT Press; 2003.

[32] Beer G. Programming the boundary element method. An introduction for engineers. New York: John Wiley; 2001.

[33] Martinod J, Hatzfeld D, Savvaidis P, Katsambalos K. Rapid N–S extension in the Mygdonian Graben (Northern Greece) deduced from repeated geodetic surveys. Geophys Res Lett 1997;24:3293–6.

[34] Riepl J, Bard P-Y, Hatzfeld D, Papaioannou C, Nechtschein S. Detailed evaluation of site-response estimation methods across and along the sedimentary Valley of Volvi. Bull Seism Soc Am 1998;88:488–502.

[35] Makra K, Raptakis D, Chávez-García FJ, Pitilakis K. Site effects and design provisions: the case of Euroseistest. In: Roca A, Oliveira C, editors. Earthquake microzoning. Pure Appl Geophys 2001;158:2349–67.